LARGE-SCALE STRENGTH TESTING OF HEXCRETE SEGMENT DESIGNED WITH UHPC FOR TALL WIND TURBINE TOWERS

Robert Peggar (1) and Sri Sritharan (1)

(1) Iowa State University, Ames IA

Abstract

To overcome the transportation and logistical challenges of using traditional land-based steel wind turbine tower designed with hub heights of 100 m (328 ft) and higher, Iowa State University (ISU) developed a precast concrete wind tower known as the Hexcrete tower. The Hexcrete tower is a hexagonal shaped, precast concrete concept developed for tall towers using both High Strength Concrete (HSC) and Ultra-High Performance Concrete (UHPC). This tower technology was further advanced with sponsorship from the U.S. Department of Energy (DOE) and a proof test of a full-scale section of a 120-m Hexcrete tower was designed, fabricated, and tested. The test unit successfully withstood both operational and extreme loads as a single system despite being formulated from prefabricated HSC and UHPC elements. In this paper, the preliminary results of the experimental study are discussed, including comparison of HSC and UHPC member performance, benefits of UHPC, and opportunities to further increase wind tower height.

Résumé

Pour pallier les difficultés de transport et de logistique associées aux traditionnels mâts d'éolienne terrestres en acier, pour des hauteurs de plus de 100 m, l'université de l'Etat d'Iowa a développé un système de mât d'éolienne « Hexcrete Tower » en éléments hexagonaux de béton préfabriqué. Ce système a été développé pour les mâts de grande hauteur et utilisant du béton à hautes et ultra-hautes performances. La technique a été améliorée avec le soutien du Ministère fédéral de l'énergie, et une épreuve sur un tronçon à l'échelle un d'un mât « Hexcrete » de 120 mètres de haut a été conçue et réalisée. L'élément prototype a résisté aux charges de service et aux charges extrêmes et conservé son intégrité bien qu'il soit constitué d'éléments préfabriqués de béton à hautes performances (BHP) et de BFUP assemblés. L'article analyse les premiers résultats de ces essais, en comparant les performances structurelles des éléments en BHP et en BFUP, les avantages du BFUP, et les possibilités pour augmenter la hauteur des mâts des éoliennes.

1. INTRODUCTION

Tall wind turbine towers provide many benefits for energy production when compared to the currently available tower technologies. Wind speeds increase with height and are less affected by natural or manmade terrain. Higher wind speeds translate to power production by a cubic relationship, which allows a significant increase in power production from a moderate increase in hub height. Larger towers also facilitate the opportunity to utilize longer blades to further increase production rates. In addition, some areas of the U.S., which do not utilize wind power due to minimal low level wind resources, would be able to generate wind power at higher heights (National Renewable Energy Laboratory, 2016). Therefore, a cost-effective tall wind turbine tower solution has the opportunity to dramatically increase U.S. energy production.

The current wind tower market in the U.S. and several other countries is dominated by the 80 m (260 ft) tall steel shell tower. However, at higher hub heights, steel shells face limitations. The 80 m steel tower base is typically around 4 m (13.5 ft) in diameter, but a 100-m tall tower would require the base to grow to 5.5 m (18 ft) in diameter if the same material properties are used (Lewin & Sritharan, 2010). The larger base prohibits cost-effective transportation due to the height of highway overpasses and lane widths. Steel shells can increase in thickness instead of growing in diameter, but this would result in almost doubling the volume of steel even for 100 m tall towers, significantly increasing material costs (Lewin & Sritharan, 2010). For these reasons, precast concrete shell towers have begun to be implemented in Europe and South America (Acciona WindPower, 2016). Concrete shells are cast in smaller segments than circular steel tower sections, typically combining three to four shells, which are joined together to make a full circular cross-section. The precast shells may require larger upfront cost due to the specialized formwork, but offer improved transportation options while using readily available concrete materials. Due to the use of reduced strength of concrete compared to steel, concrete towers often require large amounts of material, increasing the tower weight.

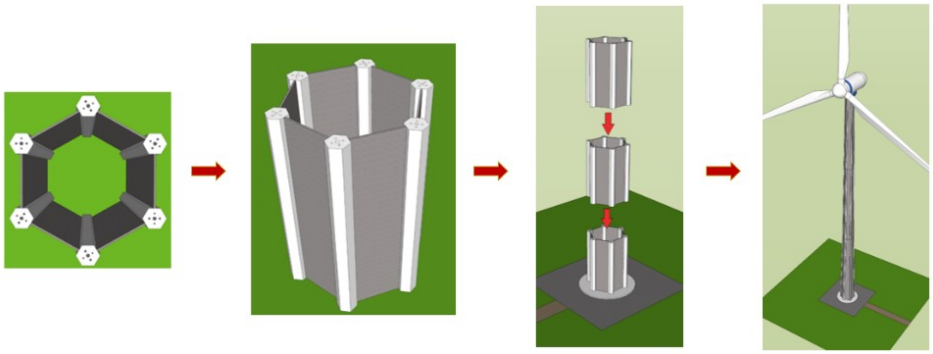

Figure 1: Hexcrete wind tower concept

To fully realize the benefits of concrete towers, the Hexcrete concrete technology (U.S. Patent No. 9,016,012, 2015) (U.S. Patent No. 8,881,485, 2014) was developed by Iowa State University. The Hexcrete tower is a hexagonal shaped concrete tower that utilizes high strength concrete materials and precast concrete shapes that do not require curved sections or costly specialized formwork. Additionally, the tower consists of six hexagonal shaped columns and six flat wall panels that serve to connect the columns as shown in Figure 1. The columns and panels are linked by unbonded radial post-tensioning, while unbonded vertical post-tensioning

runs through the columns to secure the tower to the foundation and provide structural continuity. The tower elements are made out of a combination of Ultra-High Performance Concrete (UHPC) with a compressive strength of 179.3 MPa (26 ksi) and High Strength Concrete (HSC) with a compressive strength of 89.6 MPa (13 ksi). Multiple Hexcrete towers were designed for hub heights at both 120 m (394 ft) and 140 m (459 ft) with sponsorship from the U.S. Department of Energy and Iowa Department of Energy, with in-kind contribution from LaFarge North America. Industry partners for the project included Siemens Corporate Technology, BergerABAM, Coreslab Structures of Omaha, and the National Renewable Energy Labs (NREL).

To validate the Hexcrete design methodology and further evaluate tower performance, a proof test of a full-scale tower segment was designed and tested at the Multi-Axial Subassemblage Testing (MAST) Laboratory in Minneapolis, Minnesota. In the following sections, the design and fabrication of the test unit is described as well as instrumentation and loading details. The goal of the test was to evaluate the strength of a critical Hexcrete tower segment under both operational and extreme loads. For design of wind towers, fatigue loads resulting from the dynamic response of the tower can also govern aspects of design. Therefore, a separate fatigue test was conducted at Iowa State University with results that will be published in the future. The MAST test provided an opportunity to evaluate the tower performance in regard to strength and stiffness, connection and system integrity, and member and overall tower segment behavior when subject to combined moment, shear, axial, and torsional loads representing actual loads from a 2.3 MW turbine.

2. TEST UNIT DESIGN

The test unit was designed as a full-scale section of a 120-m tower housing a 2.3 MW-108 Siemens turbine; it replicated the geometry of a tower section located at a height of 105 m (345 ft). This part of the tower was chosen based on the magnitude of the tower loads and the loading capacity of the MAST laboratory. The test unit section was 5 m (16.5 ft) tall and 2.4 m (8 ft) in diameter at the centerline. The height of 5 m was selected based on crane weight limitations within the laboratory. The overall dimensions of the test unit are shown in Figure 2. The test unit utilized both HSC and UHPC in order to validate the performance of each material in the Hexcrete tower system. Three columns and three panels were designed to be HSC members and the other three columns and panels were UHPC members. Using HSC and UHPC also offered the opportunity to directly compare the performance of each material throughout testing.

To increase structural capacity and provide economical connections between members, the Hexcrete tower consists of both radial and vertical unbonded post-tensioning. The radial post-tensioning of the tower was not designed to be installed around the entire tower circumference. Instead, the radial tendons were divided into two overlapping groups in order to reduce the number of curves in each tendon as shown in Figure 3. The radial post-tensioning in the test unit consisted of 14 groups of four 15.24 mm (0.6 in.) diameter, 1861 MPa (270 ksi) low relaxation tendons, which translated to seven circumferential groups of tendons along the test unit height with an average spacing of 0.69 m (2.25 ft) (Figure 3). The 120-m Hexcrete tower was designed with one set of vertical post-tensioning tendons per column, which extend the entire height of the tower. The critical design section for determining the number of tendons in a single column is typically located at the base of the tower, which results in reserve capacity at higher tower elevations. Since the test unit section was located at a height of 105 m, the

number of vertical tendons in the test unit was reduced from the original tower design in accordance with the capacity demands at the base of test unit. This resulted in a group of twenty tendons in each column of the test unit.

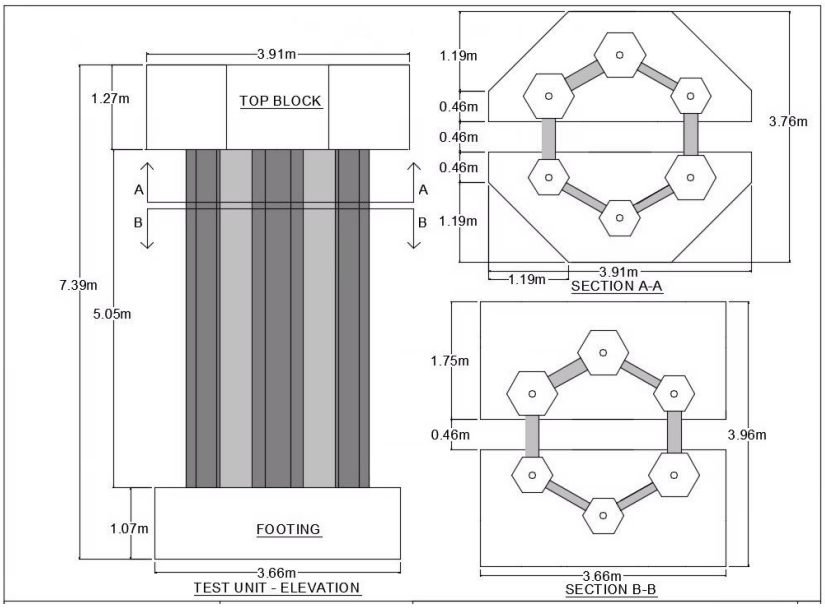

Figure 2: Test unit schematic

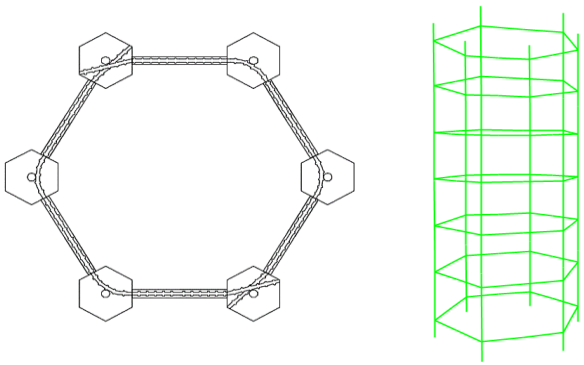

Figure 3: Radial tendon layout (left);
radial and vertical tendon locations along test unit height (right)

Foundation blocks and top reaction blocks were designed to anchor the vertical post-tensioning and also to attach the tower test section to the strong floor and loading crosshead, respectively. The depth of each block was determined by the space necessary to ensure proper anchorage of each set of post-tensioning tendons. All post-tensioning anchorage locations for tendons in the Hexcrete tower and test unit were designed to follow code requirements for allowable stress limits from the American Concrete Institute (ACI), namely the concrete stress limit of 0.45f'c specified for sustained load conditions. The vertical tendons used in the test unit design were 1861 MPa low-relaxation seven-wire tendons.

3. TEST UNIT CONSTRUCTION

The precast concrete pieces for the test unit were fabricated at Coreslab Structures in Omaha, Nebraska and shipped to the MAST laboratory. The test unit was constructed in two halves due to space and lifting limitations within the test facility. Each half consisted of a single foundation block, three columns, two panels, and a single top block. This construction approach did not benefit the two panels that would connect the test unit halves, since the panels would not be subject to precompression from the vertical post-tensioning, but was necessary due to laboratory limitations. A temporary support frame was constructed to hold the columns and panels in place during the construction process. Prior to positioning the columns on the foundation, grout forms and steel shims were placed at the column locations for grouting the column-to-foundation interface. The columns were set in place on the steel shims and attached to the support frame. The grout pads were not poured at this time in order to allow adjustment of the columns during placement of the two connecting wall panels. These panels were then positioned between the columns and attached to the support frame for stability. The tower segment was designed with a 20 mm (0.75 in.) gap between each column and panel to allow for construction tolerances. High strength epoxy was applied in this gap in order to provide a uniform bearing surface for radial post-tensioning. The epoxy was mixed and then manually packed into the joints between the columns and panels using trowels. No compression force was applied to the joint during the curing process. After curing of the epoxy, six 12.70 mm (0.5 in.) diameter tendons were utilized to temporarily connect the columns and panels. Two tendons were placed through the top, middle, and bottom of the half test unit and subsequently tensioned to an effective stress of 868 MPa (126 ksi) per tendon. The half test unit was not yet permanently attached to the foundation block, but the self-weight of the pieces and the support frame kept the members in place during the temporary radial tensioning. Grout pads were then poured at the top of the columns, the top block was set in place, and the vertical post-tensioning tendons were installed. At this time, the grout pads at the base of the columns were also poured. After all the grout pads were sufficiently cured, the vertical post-tensioning was tensioned to an effective stress of 1124 MPa (163 ksi) per tendon and the support frame was removed. The half test unit was then lifted into its final position for testing and attached to the MAST strong floor. The second half of the test unit was constructed using the same method, moved into the correct position and attached to the strong floor as well.

After both halves of the test unit were attached to the strong floor, the temporary post-tensioning between the columns and panels was removed, the final two panels were placed, and epoxy was installed at the column interfaces for these two panels. After curing of the epoxy, radial 12.70 mm diameter post-tensioning tendons were run through the columns and panels to connect the entire unit and tensioned to an effective stress of 1145 MPa (166 ksi) per tendon. The original tower design included 15.24 mm diameter tendons instead of the 12.70 mm. However, placement of the 15.24 mm tendons in the test unit was not possible due to the curvature of the post-tensioning ducts combined with the duct's corrugated inner surface. Although this challenge can be easily overcome in a prototype tower by using larger ducts, 15.24 mm tendons were substituted with 12.70 mm tendons in the test unit, and the panel stresses and joint interface forces were reexamined to understand how the smaller tendons would affect the test unit capacity. It was calculated that the smaller tendons could result in a weaker interface between the columns and panels and possibly allow premature panel cracking due to lower precompression. After completion of the radial post-tensioning, the test unit was attached to the testing crosshead to allow load application.

4. INSTRUMENTATION

To adequately capture the test unit behavior, an extensive instrumentation scheme was used. Four types of instruments were used to collect test data: strain gages, string potentiometers (string pots), Linear Variable Displacement Transducers (LVDTs), and an Optotrack 3D camera system. Strain gages were placed on rebar at the precast plant near post-tensioning locations in order to monitor the effects of the vertical post-tensioning on the foundation and top blocks. Concrete strain gages were also placed on the surface of two concrete panels (one HSC and one UHPC) to monitor and compare stresses in the panels. String pots were attached to four of the test unit columns in order to record the overall test unit displacement. LVDTs were placed in order to measure displacement at the column to panel connections as well as between the columns and the foundation and top blocks. The Optotrack camera system measured panel stresses on a UHPC panel to compare with the concrete strain gage stress readings.

5. TEST UNIT LOADS

A loading protocol was formulated to investigate the tower section behavior under operational and extreme loads. Three design load cases (DLCs) as defined by the International Electrotechnical Commission (IEC) 61400-1 were considered in order to accurately simulate the maximum operational and extreme forces experienced by the tower section. Each load case included a shear force, overturning moment, axial force, and torsional moment. The first load case was IEC DLC 1.1, where the resultant loads are caused by atmospheric turbulence under normal tower operation (IEC, 2008). This load case generates the largest tower overturning moment for both operational and extreme load conditions. The second load case was IEC DLC 4.2, which corresponded to the wind turbine switching from power production to idle or stand still (IEC, 2008). The change in position generates the largest tower shear force at operational and extreme loads. The last load case was IEC DLC 2.2, which corresponded to an electrical fault in the control protection system and results in the largest tower torsional moment at operational and extreme conditions (IEC, 2008).

6. TEST RESULTS

Following the construction and instrumentation of the test unit, the loading process was initiated. For both operational and extreme loads, two critical parameters were identified to evaluate the response of the tower test section. The first parameter was the stiffness of the tower section during loading, which was defined in terms of the load versus displacement response of the structure. The test unit was designed to remain elastic under both operational and extreme loads. The second critical response parameter was concrete cracking in the test unit members including both the crack location and crack size. Although the test unit was designed to remain uncracked under operational and extreme loads, the reduction in horizontal post-tensioning could influence this response.

Operational loads were the first set of loads applied to the test unit. For each load case the loads were applied in 25% increments until the full load was reached. The operational loads corresponding to DLC 1.1 and 4.2 were applied with no observable damage and small amounts of deflection. For the torsional loading of DLC 2.2, the test unit responded in a linear manner (Figure 4); however, hairline cracks were observed on all the HSC panels at 100% load. The two HSC panels, which connected the two test unit halves during construction, experienced

moderate amounts of cracking as shown in (Figure 5) while only a single crack appeared in the third HSC panel. These cracks, which were marked with a black marker for visibility, did not exceed a width of 0.1 mm (0.004 in). No further damage was observed under operational loads. The cracks also completely closed upon unloading of the test unit.

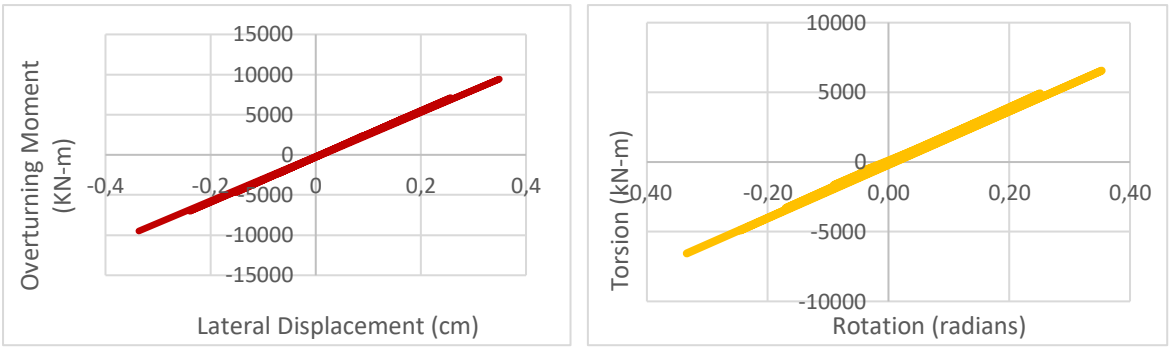

Figure 4: Operational lateral (left) and torsional (right) displacements

Figure 5: Cracking of the two HSC connecting panels after completion of operational torsional loading

As previously stated, the HSC panels were not designed to crack under operational torsional loads. After further investigation of the data collected from the panel instrumentation, it was determined that the construction sequence and use of smaller radial tendons were both responsible for the observed cracking. The vertical post-tensioning introduced a larger amount of precompression in the panels than was predicted before the test and this precompression was not present in the connecting panels. The reduction in radial post-tensioning also contributed to the panel cracking in contrast to the calculations performed at the time of construction.

After completion of the operational loads, extreme load values were applied to the test unit. No damage occurred in the test unit when loads for DLC 4.2 and DLC 1.1 were applied and the test unit continued to behave in an elastic fashion (Figure 6). At 75% application of the extreme torsional load (DLC 2.2), new 0.1 mm cracks were observed on the base of one of the two HSC connecting panels as shown in Figure 7. The original cracks that occurred during operational loading, increased in width to 0.2 mm (0.008 in.). Additional 0.1 mm cracks also appeared on the connecting HSC panels at 100% extreme torsional load, a single new crack appeared at the base of the third HSC panel, and 0.1 mm cracks formed on one of the UHPC columns. The cracks on the UHPC column were localized around a radial PT anchorage location as shown in

Figure 7 which appears to lack steel fibers in the UHPC at this location. These type of cracks did not appear in any other columns, which reinforces the idea that the problem was a local issue. UHPC fiber distribution can be improved by reducing the amount of reinforcement in the columns and based on the observed performance of the test unit, it is expected that the column reinforcement can be reduced. It is also important to note that the panel cracking was limited to HSC panels and that UHPC panels did not experience cracking under torsional loads. The absence of cracks in the UHPC panels is due to the higher tensile capacity of UHPC. After applying 100% of the extreme torsional load DLC 2.2, the force-displacement response of the test unit continued to be linear with no decrease in strength. As was the case for operational loads, all cracks closed completely when the loads were removed from the test unit and no further damage was observed.

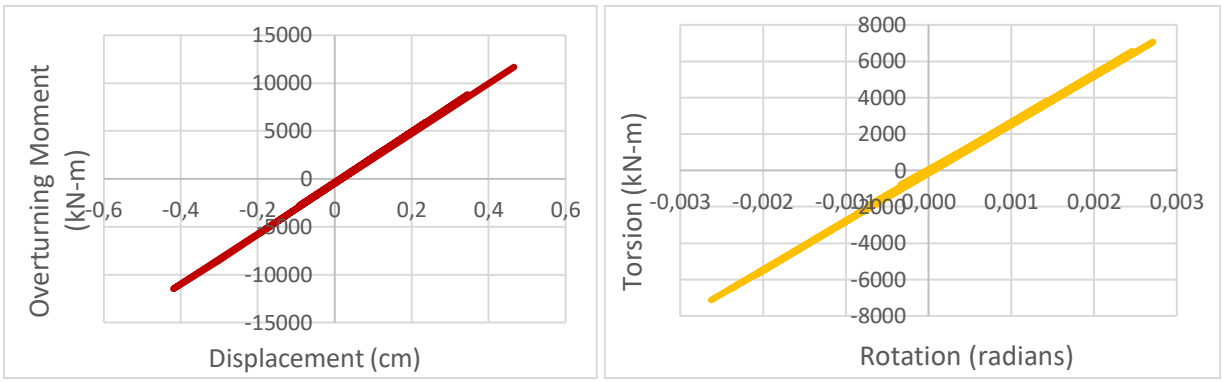

Figure 6: Extreme load lateral (left) and torsional (right) responses

Figure 7: Torsional cracking under extreme torsional loads (left) UHPC column cracking (right)

Since the test unit force-displacement response remained linear after the application of extreme loads, large magnitude loads were applied in order to measure the full capacity of the unit and also identify the failure mechanism of the tower system. To reach the test unit capacity, loads corresponding to the operational and extreme design envelopes were applied. The design envelopes were a combination of all three load cases originally applied to the test unit. A small number of 0.1 mm cracks were observed on the HSC connecting panels under the operational load envelope, but no further damage or change in stiffness was observed during the lateral and torsional test unit responses. However, at the extreme envelope loading, a drop in torsional

stiffness was observed due to further cracking of the connecting HSC panels and separation in the epoxy joints between multiple UHPC panels and the test unit columns.

The test unit retained a large amount of load capacity after the decrease in stiffness, and therefore, torsional displacements were continuously applied in increasing magnitude beyond the extreme load envelope. Damage to the test unit progressed steadily as the torsional displacement increased beyond 0.017 radians (1 degree) of rotation (0.017 radians of rotation was five times the rotational displacement for extreme torsional loading). Both HSC and UHPC columns experienced torsional cracking, new cracks continued to appear on the HSC panels, and the epoxy between all of the column and panel connections began to crack or split vertically. The UHPC panels did not experience visible cracking, but gaps up to 6.35 mm (0.25 in.) opened between the UHPC panels and columns at the epoxy joint. At 0.07 radians (4 degrees) of rotation, spalling had occurred on both HSC and UHPC columns and the test was terminated due to damage to the foundation blocks. The progression of damage to the test unit during the large displacement cycles is shown in Figure 8 as well as the tower rotational displacement response. The test unit was still able to support the axial load simulating the weight of the nacelle and rotor after the completion of testing. The response of the test unit showed that the tower had sufficient ductility beyond extreme loads.

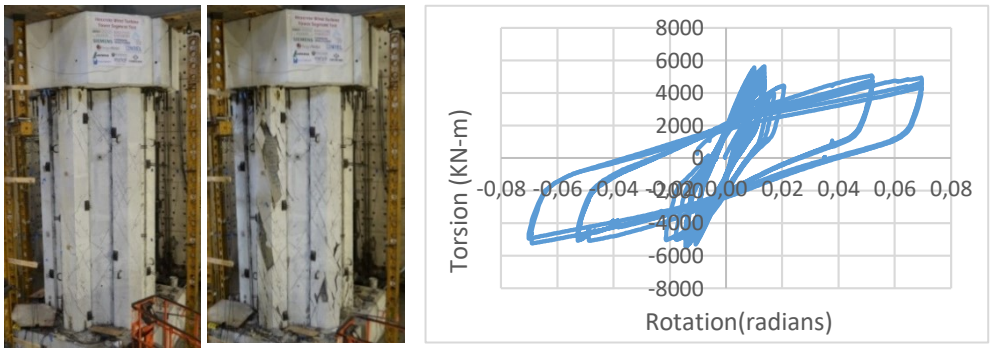

Figure 8: Large displacement damage (left) and response (right) of test unit

7. CONCLUSION

The primary objective of the Hexcrete unit test was to validate strength capacity of the tower design process and demonstrate the integrity of the assembled tower section in resisting both the operational and extreme loads in an elastic manner. Based on the operational and extreme load performance of the test unit, it can be concluded that the test unit did act as a single unit and remained elastic through both operational and extreme loads. Premature cracking of the test unit was observed on the connecting panels as the result of the test unit construction sequence dictated by the laboratory limitations and use of smaller radial tendons. Both issues will be eliminated in prototype construction of the tower system since the entire Hexcrete cross-section is built and stacked before vertical post-tensioning is applied and larger ducts can be utilized for the radial tendons. The UHPC panels in the test unit did not experience any cracking through the operational and extreme loading cycles. Localized cracking also occurred at one UHPC column anchorage location and was due to lack of steel fiber distribution in UHPC. This cracking can be prevented with proper casting procedures. In summary, despite premature cracking, no loss in strength or change in tower stiffness occurred in either the lateral or torsional tower response for both operational and extreme loads. The tower section continued to carry axial load and maintained

structural integrity after the application of large torsional displacement cycles. The test results validate the strength capacity of the Hexcrete tower system and through a corresponding cost analysis; UHPC was selected as the preferable panel material for the Hexcrete towers. When these results are combined with proven fatigue performance and completed cost analyses, the Hexcrete tower technology is a suitable option for tall wind turbine towers.

ACKNOWLEDGEMENTS

The information, data, or work presented herein was funded in part by the Office of Energy Efficiency and Renewable Energy, U.S. Department of Energy, under award number DE-EE0006737 (http://sri.cce.iastate.edu/hexcrete/). Additional funding and in-kind support were obtained from Iowa Energy Center and Lafarge North America Inc. of Chicago, Ill., respectively. Members of the project team are listed at the project website. The authors also thank industry partners who participated in workshops focused on Hexcrete tower production, estimating, construction, and erection costs. The participants included Kevin Dieter of Pattern Energy, Jon Grafton of Oldcastle, David Dieters of Midstate Precast, Ken Fleck of Patterson, Daniel Harger of Structural Technologies VSL, Mark Strzok of Bigge Crane and Rigging, Kirk Morgan of Barr Engineering, and Dan Juntunen and Tim Edland of Wells Concrete.

REFERENCES

[1] National Renewable Energy Lab. (2016, June). *NREL Wind Resources*. Retrieved from http://www.nrel.gov/wind/news/2015/19541.html
[2] Lewin, Thomas James, "An investigation of design alternatives for 328-ft (100-m) tall wind turbine towers" (2010). *Graduate Theses and Dissertations.* Paper 12256.
[3] Acciona Wind Power. (2016, June). *Concrete Towers*. Retrieved from http://www.acciona-windpower.com/technology/concrete-towers/
[4] Sritharan, S., T. Lewin, and G. M. Schmitz. 2014. Wind turbine tower systems. U.S. Patent 8,881,485, filed May 13, 2014, and issued November 11, 2014.
[5] Sritharan, S. and T. Lewin. 2015. Wind turbine tower systems. U.S. Patent 9,016,012, filed May 23, 2012, and issued April 18, 2015.
[6] IEC, I. E. (2008). *IEC 61400-1: Wind Turbines - Part 1: Design Requirements (3rd Edition).* International Electrotechnical Commission.

DISCLAIMER